Available online at www.sciencedirect.com
SCIENCE DIRECT®
Journal of Solid State Chemistry 177 (2004) 251–256
JOURNAL OF SOLID STATE CHEMISTRY
http://elsevier.com/locate/jssc

The combustion synthesis of iron group metal fine powders

J.H. Lee,* H.H. Nersisyan, and C.W. Won

Industries Lab, Rapidly Solidified Materials Research Center Sierra (RASOM), Chungnam National University, 220 Kungdong, Yuseong, Daejeon 305764, South Korea

Received 25 May 2003; received in revised form 1 August 2003; accepted 2 August 2003

Abstract

The new approach has been developed for the synthesis of nickel (Ni), cobalt (Co) and iron (Fe) powders from the appropriate oxides by the solid combustion method. The reduction was made by sodium azide (NaN_3) at the presence of carbon in the argon atmosphere. The variation of combustion temperature and velocity was performed by using alkali metal salt as an inert diluent. The values of combustion parameters were measured and also the temperature distribution in a combustion wave are obtained. The geometric sizes of reactionary zones and the activation energy of the process were estimated. The optimum conditions for single-phase metal powder synthesis were found. Powders fabricated in this way had cubic structure and particles size about 0.5–2.0 μm for Ni, Co and 1–3 μm for Fe. In a number of cases the formation of spherical particles with the average size about 5–15 μm were observed.

Keywords: Combustion synthesis; Iron group; Inert diluent

1. Introduction

Iron group metals (Fe, Co, Ni) are of great importance in the industry. They have been widely used in the pure state as well as in the composition of various alloys. Nowdays ultrafine powders of these metals having uniform shape and high purity are increasingly required for specific uses in many technological areas, such as Base Metal Electrode Multilayered Ceramic Capacitor (BME-MLCC) industry for personal computers, cellular phones, and other electronic devices, chemical industry—as catalyst and other. A variety of techniques have been used to produce pure metals such as, chemical reduction [1,2], gas evaporation [3,4], ball milling [5], sol–gel process [6,7], sonochemical [8], etc. Because all the above applications require fine metallic powders, an alternative inexpensive and simple method for producing such powders is of considerable interest. One possible approach is to prepare the powders by combustion synthesis [9–11].

Advantages of the combustion synthesis in comparison with another ones are small energy consumption for the achievement of high temperatures, high rates of synthesis, the simplicity of equipment and high quality of final products. Ultrafine powders of several metals have been synthesized by combustion synthesis; titanium [12], tantalum [13], tungsten [14,15]. In all cases the synthesis was carried out from appropriate oxides with use of magnesium as reduction agent. To our knowledge the production of the powders of iron group metals by combustion synthesis has not been reported in the literature.

The purpose of this study is to describe a new simple way for the preparation of metallic Ni, Co and Fe fine powders by combustion processes using inexpensive metal resources (metal oxide) and as a reducing agent sodium azide combinated with carbon. Single phase nickel, cobalt and iron powders have been obtained and characterized herein.

Sodium azide as solid source of nitrogen is common in the combustion field [16,17]. It has been also widely used for the preparations of transition metal nitrides via combustion like rapid metathesis reaction [18,19]. But an alkali metal azide was not considered as reduction agent in combustion synthesis, because it contains large quantity of nitrogen. In the case of iron group metals the formation of nitride phase can be excluded, thus the combustion reaction leads to the formation of pure metal.

*Corresponding author. Fax: +82-42-822-9401.
E-mail address: jong-lee@cnu.ac.kr (J.H. Lee).

0022-4596/$ - see front matter © 2003 Elsevier Inc. All rights reserved.
doi:10.1016/j.jssc.2003.08.003

2. Experimental

The raw materials used in this study were: NiO, Co_3O_4, Fe_3O_4, NaN_3, NaCl, granulated black carbon (<0.1 μm) (99.5% purity, Samchun Pure Chemical Co. LTD, Korea), and argon gas (99.9% purity). Appropriate amounts of metal oxide, sodium azide, black carbon and sodium chloride were mixed in the ceramic mortar at room temperature. Preliminary the initial mixture was stamped into the cylindrical metallic mould from stainless steel with the 2 mm thickness, 30 mm diameter and 40 mm in height. Experimental densities of samples were 1.5–1.7 g/cm^3. During a typical experiment the pellet is placed into a constant pressure reactor and the reaction is initiated by means of a nickel-chromium wire connected to the power supply, which was programmed to produce an energy pulse by setting 15–20 V for about 1.0–1.5 s. The combustion was carried out in argon atmosphere at the pressure of 0.5 MPa.

The maximum combustion temperature (T_c) and temperature distribution were measured by tungsten-rhenium thermocouples (W/Re-5 vs. W/Re-20) with 100 and 50 μm in diameter previously covered with alumina thin layer and embedded in the center of the sample at predefined distances from each other.

The input signals of thermocouples were transformed by data logger (DASTC) at the rate of 10 Hz, and were recorded by computer. The average values of combustion velocity are as follows: $U_c = l/t$, where U_c is the combustion velocity; l is the distance between thermocouples; and t is the temporary time between signals of thermocouples. The standard error of measurement for T_c and U_c were $\pm 25°$ and 5%, respectively.

The phase composition of the combustion products was determined by X-ray diffractometer (XRD; Siemens D5000, Germany). The morphology of products and mean particle sizes were determined by scanning electron microscopy (SEM) (JSM 5410, Japan). Thermogravimetric and differential thermal analyses (TG-DTA) were performed under air or argon atmosphere, respectively, at heating rate of range 10–20°C/min.

3. Results and discussion

The investigation was carried out on the Me_xO_y–NaN_3–C–NaCl system, where Me_xO_y is NiO, Co_3O_4 and Fe_3O_4. The reduction of metal oxides was performed by sodium azide combinated with carbon. Total process of reduction can be described by the following equation:

$$Me_xO_y + 2y/3NaN_3 + y/3C = xMe + y/3Na_2CO_3 + yN_2. \quad (1)$$

3.1. Thermodynamics of process

The preliminary thermodynamic analyses of the NiO–$0.67NaN_3$–0.335C, Fe_3O_4–$2.7NaN_3$–1.35C and Co_3O_4–$2.7NaN_3$–1.35C stoichiometric mixtures in the presence of NaCl as an inert diluent were performed by the program "THERMO" [20]. Calculation of equilibrium characteristics is based on minimizing the thermodynamic potential which expression accounts for the contributions of thermodynamic potentials for all the components present in the system.

As a typical example the diagram of adiabatic combustion temperature and equilibrium composition of combustion products in NiO–$0.67NaN_3$–0.335C–kNaCl (where k is mol-number of NaCl) system is given in Fig. 1. As one can see thermodynamically possible products of combustion reaction are metallic nickel and sodium carbonate. The adiabatic combustion temperature (T_{ad}) is maximum at $k = 0$ and makes 1352 K. It is obvious that T_{ad} can be lower by the addition of NaCl in the initial mixture as an inert diluent that creates milder conditions for combustion and phase formation. In this figure, the changes of enthalpy (ΔH) and entropy (ΔS) of final products are also presented, and they increase with increase of k. The similar thermodynamic situation was recorded for the cobalt and iron containing systems. The values of T_{ad} obtained from the thermodynamic calculation are given in Table 1.

3.2. The combustion laws of Me_xO_y–NaN_3–C–NaCl system

Two typical parameters of combustion reaction were measured during the experiment: velocity of wave propagation and combustion temperature. The curves reflecting the relation between these two parameters are shown in Fig. 2. The changes of combustion parameters

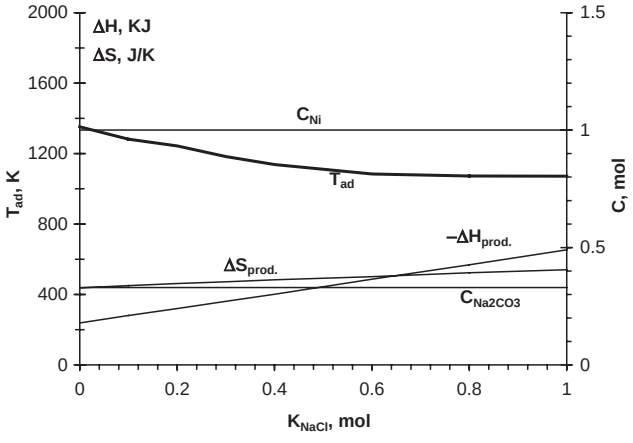

Fig. 1. Diagram of adiabatic combustion temperature and equilibrium composition of combustion products in NiO–$0.67NaN_3$–0.335C–kNaCl system, $T_o = 298$ K, $P_o = 0.5$ MPa.

Table 1
Combustion characteristics of $NiO + NaN_3 + C +$ inorganic salt systems

No.	Green mixture	T_c (K)	T_{ad} (K)	U_c (cm/s)	Phase composition
1	$NiO–0.67NaN_3–0.335C$	1390	1352	0.4	Ni(f.c.c.)
2	$NiO–0.67NaN_3–0.335C–0.3NaCl$	1195	1183	0.13	Ni(f.c.c.), NiO (5 wt%)
3	$NiO–0.67NaN_3–0.335C–0.5NaCl$	1080	1122	0.08	Ni(f.c.c.), NiO (<10 wt%)
4	$NiO–0.67NaN_3–0.335C–0.7NaCl$	990	1073	0.048	Ni(f.c.c.), NiO (<15 wt%)
5	$NiO–0.4NaN_3–0.4C$	1070	1023	0.17	Ni(f.c.c.), NiO (<20 wt%)
6	$Co_3O_4–2.7NaN_3–1.35C$	1770	1466	0.34	β-Co(f.c.c.)
7	$Co_3O_4–2.7NaN_3–1.35C–1NaCl$	1270	1314	0.12	β-Co(f.c.c.)
8	$Co_3O_4–2.7NaN_3–1.35C–2NaCl$	1070	1185	0.073	β-Co(f.c.c.), Co (h.c.p.)
9	$Co_3O_4–2.7NaN_3–1.35C–3NaCl$	950	1130	0.042	β-Co(f.c.c.), α-Co (h.c.p.), CoO (<10 wt%)
10	$Fe_3O_4–2.7NaN_3–1.35C$	1170	1130	0.11	α-Fe(b.c.c.)
11	$Fe_3O_4–2.7NaN_3–1.35C–0.5NaCl$	1090	1090	0.08	α-Fe(b.c.c.)
12	$Fe_3O_4–2.7NaN_3–1.35C–NaCl$	1000	1060	0.065	α-Fe(b.c.c.), FeO (<10 wt%)
13	$Fe_3O_4–2.7NaN_3–1.35C–1.5NaCl$	900	1042	0.04	α-Fe(b.c.c.), FeO (<15 wt%)

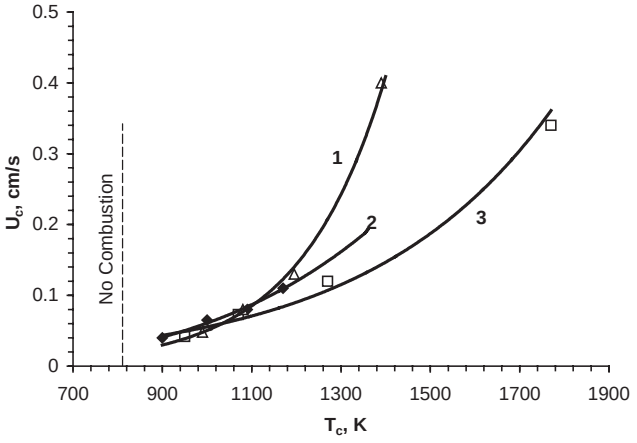

Fig. 2. The relation between T_c and U_c in $Me_xO_y–NaN_3–C–k$NaCl system, $T_o = 298$ K, $P_o = 0.5$ MPa, 1-Hi, 2-Fe, 3-Co.

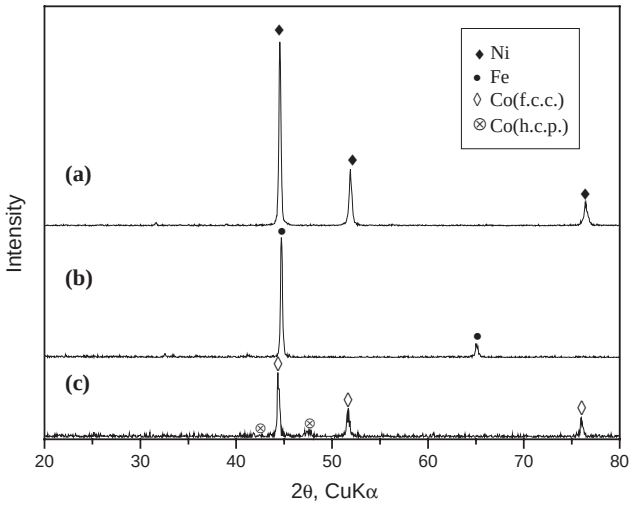

Fig. 3. Typical XRD patterns of nickel (a), iron (b) and cobalt (c) powders.

were achieved by dilution of the initial mixture. The compositions of green mixtures are given in Table 1. According to the results obtained, the dilution of green mixtures leads to simultaneous decreases of T_c and U_c. At the high degree of dilution the combustion limit observed, and the combustion temperature is below 850 K.

After combustion samples were kept up in the reactor up to complete cooling. Usual operations of washing by warm water and drying in vacuum drying furnace at the temperature 330–340 K of final products were made.

According to X-ray analysis single-phase powders of nickel, cobalt and iron were obtained in the interval of the temperature about 1200–1300 K (Fig. 3). At lower temperatures the combustion reaction, as a rule, does not complete and a certain quantity of metal oxide remains in a final product (see Table 1). It should be noted that as distinct from Ni and Fe the main β-Co (f.c.c) phase with a small quantity of α-Co (h.c.p) always is observed at the reduction of cobalt oxide. The quantity of α-Co phase considerably increases with the decreasing of the combustion temperature.

SEM studies gave a clear indication of a good state of particle dispersion. The typical microstructures of metal powders received by SEM analysis are shown in Fig. 4. The sizes of these powders estimated from the micrographs are in the range of 0.5–2 μm for Ni and Co and 1–3 μm for Fe. The typical image (Figs. 4a and b) demonstrates that the nickel and cobalt particles are partially spheroidal in shape and the degree of particle agglomeration is relatively low. The average sizes of the agglomerates are less than 5 μm. In comparison with the Ni and Co the particles of Fe have the form of well-defined crystals and low degree of agglomeration (Fig. 4c).

It is worth also to note that under a certain condition, the combustion process is able to lead to the formation of metal particles having the ideal spherical form (Fig. 5). In particular in Fig. 5a the micrograph of the nickel powder containing a spherical particle with the particle sizes about 5–15 μm is shown. The mechanism of these particle formations remains unclear, but from

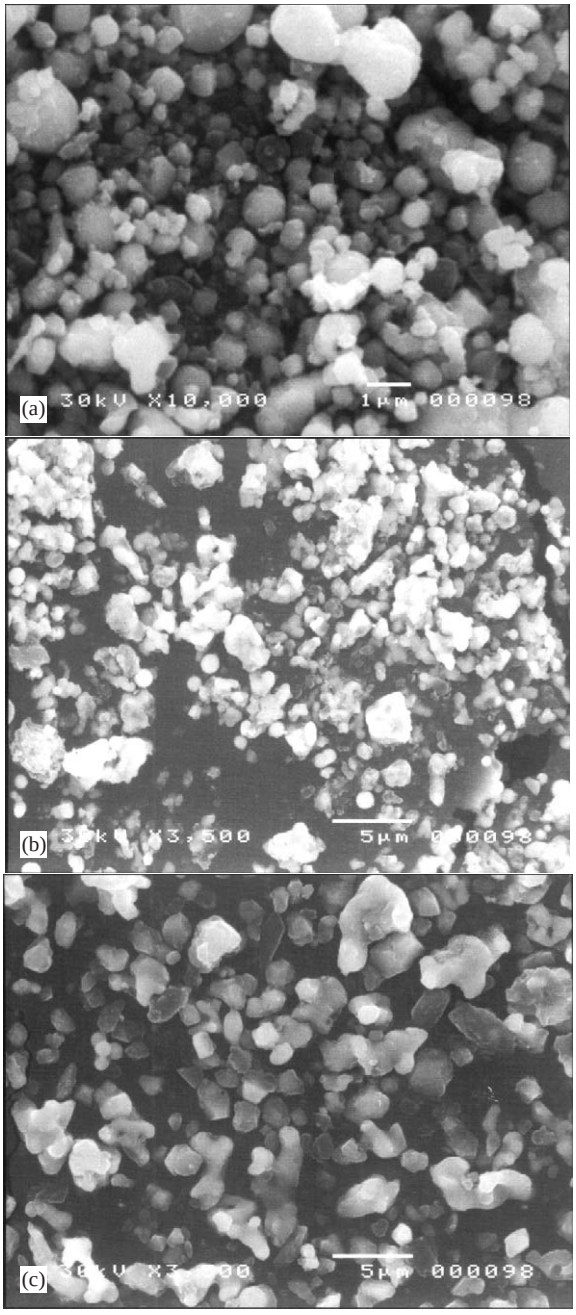

Fig. 4. SEM micrographs of nickel (a), cobalt (b) and iron (c) powders.

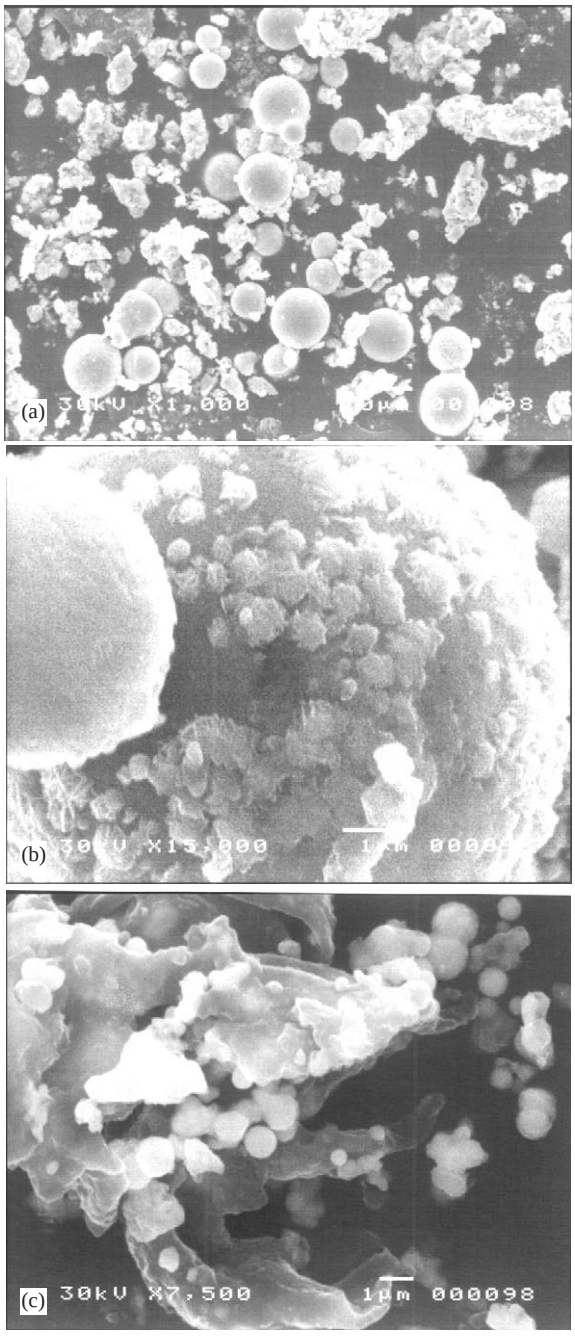

Fig. 5. Dynamics of the spherical particle formation: (a) nickel powder with spherical particles; (b) external shape of nickel particle at large magnification and (c) spherical cobalt particles with a melted shell.

an external structure of separate particles (Fig. 5b) it is possible to suppose that they are formed by consolidation of small ones. Approximately similar mechanism of spherical particle formation takes place also in the cobalt containing system (Fig. 5c).

3.3. Thermal structure of a combustion wave and kinetics of reaction

Reduction of metals from the corresponding oxides is multistage and complex chemical process proceeding at high temperatures. A lot of useful information on the process come from the measured temperature distribution in a combustion wave. In particular with their help it is possible to estimate the sizes of preheating and reactionary zones, the melting zones, leading stages of reaction and other.

The most informative and accurate technique to obtained temperature distributions is microthermocouple technique which is widely used for the description of

a combustion processes in the condensed systems [21,22].

DTA analysis of initial mixtures was carried out in an argon atmosphere to specify starting temperature of the reaction (T^*). The DTA result thus received for NiO–0.67NaN_3–0.335C mixture as a typical exemple is presented in Fig. 6. As it is visible up to 670 K initial mixture is stable and does not undergo chemical changes. At 670 K DTA analysis registers sharp exothermic peak significative, that is ignition of a mixture (T^*). This temperature corresponds to the decomposition temperature of NaN_3. There are also one endothermic area in the DTA at 1150 K which most likely corresponds to the melting of Na_2CO_3.

Temperature distributions in the combustion wave of NiO–0.67NaN_3–0.335C–kNaCl mixture at different k are given in Fig. 7. As a result of experimental research,

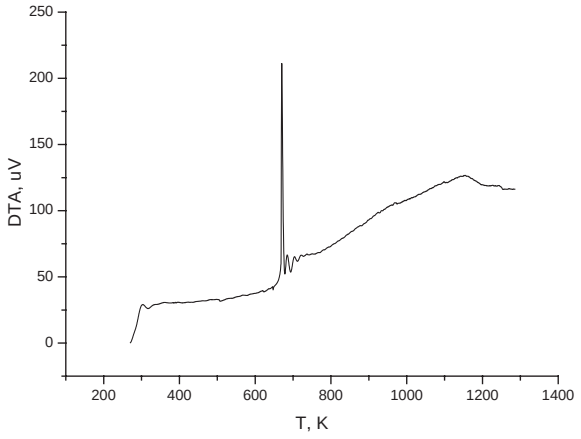

Fig. 6. DTA of NiO–0.67NaN_3–0.335C system.

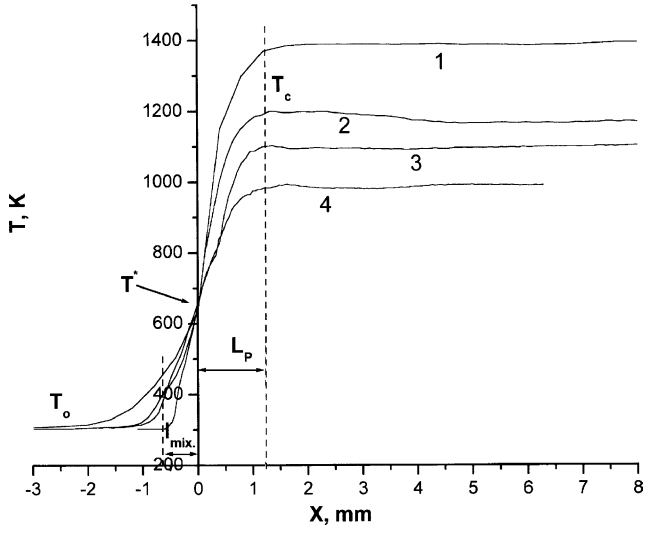

Fig. 7. Average temperature distribution in the combustion zone for NiO–0.67NaN_3–0.335C–kNaCl system: (1) $k=0$; (2) $k=0.3$; (3) $k=0.5$ and (4) $k=0.7$.

only single stage temperature distributions are revealed in the combustion wave. Here T^* is the starting temperature of reaction; L_R the thickness of the reactionary zone; and l_{mix} the thickness of the preheating zone which corresponds to the changes of temperature from T_o up to T^*. As one can see sharp increasing of the temperature takes place near to the ordinate. The difference between the sizes of preheating and reactionary zones is not high ($l_{mix}=0.75\pm0.25$ mm, $L_R=1.25\pm0.25$ mm), thus indicating about classical narrow reaction zone the concept of which were developed by Zeldovith and Frank-Kamenetsky [23]. According to this concept the combustion velocity is connected with the combustion temperature by the following equation:

$$U_c^2 = AT_c e^{-E/RT_c}. \quad (2)$$

It is obvious that the activation energy for the combustion process can be derived from the experimental values U_c and T_c in Eq. (2). For it the values of T_c and U_c were processed in coordinates $\ln U_c/T_c - 1/T_c$. The results are presented graphically in Fig. 8. The activation energies which can be extracted from the plots are: $E=$ 22, 30 and 30 kcal/mol for NiO–NaN_3–C, Co_3O_4–NaN_3–C and Fe_3O_4–NaN_3–C system, respectively.

3.4. Oxidation behavior of nickel, cobalt and iron powder

The stability of the resultant Ni, Co, Fe powders in air were characterized by thermogravimetry (TG). The heating rate of the samples was 10°C/min. The weight of the nickel powder synthesized by SHS process began to increase from around 820 K, which means the starting of oxidation as shown in Fig. 9. It seems that the Ni powder was completely oxidized to NiO at around 1270 K. The final weight gain is around 122.5% by TG that is little lower weight gain than theoretical (127.3%) value for perfect conversion of pure Ni to NiO. This datum indicates that the particles consist of pure nickel and small amount of unreduced nickel oxide.

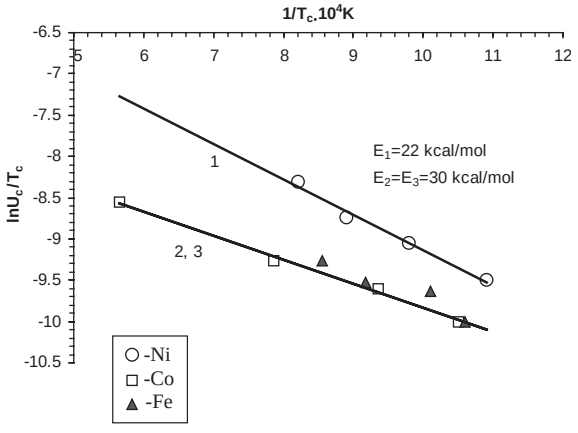

Fig. 8. Dependencies of $\ln U_c/T_c$ from $1/T_c$.

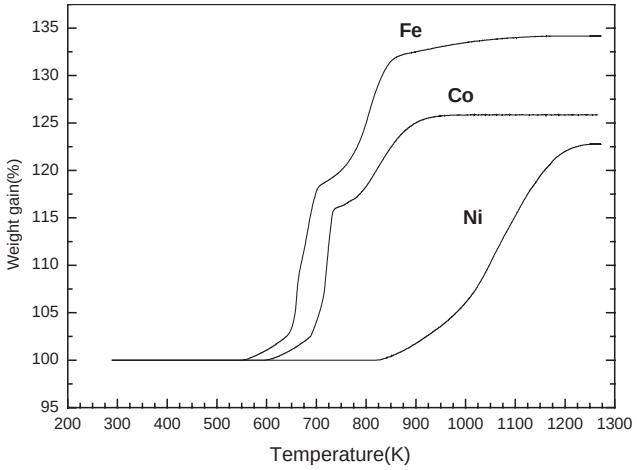

Fig. 9. TGA curves of Fe, Co and Ni powders in the air atmosphere.

The stabilities of cobalt and iron powder were found to be comparatively lower than that of nickel powder. The oxidation started from 550 to 600 K for iron and cobalt powder, respectively. Also, complete oxidation was found at around 970 K.

4. Conclusion

The most important result of this work is the development of the simple approach allowing synthesis of fine iron group metal powders by the combustion synthesis. This approach is not only limited to synthesize these metals but also to make various alloys on the basis of these metals. Also large opportunities are present for the synthesis of metals from other groups of the table of elements.

The major conclusions of this study are as follows:

1. The synthesis of iron group metals by combustion method was realized. The interrelation between the combustion temperature and wave velocity were established. It was shown that the combustion process begins after decomposition of NaN_3 at 670 K and is characterized by narrow zones of reaction. The temperature distributions on a combustion wave were constructed and activation energies of combustion processes were calculated.
2. It is shown that the received powders as a rule have cubic structure and only cobalt powder contains small amount of hexagonal phase. The average sizes of particles were made: Ni—0.5–2 μm, Co—0.5–2 μm and Fe—1–3 μm. The shapes of particles are near to spherical (Ni, Co) or well defined crystals (Fe).
3. It was established that received metals powders have a good stability to oxidation. Further work includes decreasing of unreduced oxide phase while keeping the stability to the oxidation.

References

[1] A. Degen, J. Macek, Nanostruct. Mater. 12 (1999) 225–228.
[2] S. Ayyappan, R.S. Gopalan, G.N. Subbanna, C.N.R. Rao, J. Mater. Res. 12 (1997) 398–401.
[3] L. Dong, Z. Zhang, S. Jin, W. Sun, Y. Chuang, Nanostruct. Mater. 10 (1998) 585–592.
[4] G.A. Niklasson, J. Appl. Phys. 62 (1987) 258–265.
[5] J. Huang, Y. Wu, H. Ye, Acta Mater. 44 (1996) 1201–1209.
[6] S. Roy, A. Chatterjee, D. Chakraborty, J. Mater. Res. 8 (1993) 689–692.
[7] Syukri, B. Takayuki, O. Yutaka, T. Yasataka, Mater Chem. Phys. 78 (2003) 383–391.
[8] Y. Koltypin, G. Katabi, X. Cao, R. Prozorov, A. Gedanken, J. Non-Cryst. Solids 201 (1996) 159–162.
[9] A.G. Merzhanov, Int. J. SHS 4 (1995) 323–330.
[10] Z.A. Munir, U. Anselmi-Tamburini, Mater. Sci. Rep. 69 (1989) 277–283.
[11] Y. Miyamoto, J. Mineral. Soc. Jpn. 18 (1988) 383–391.
[12] H.H. Nersisyan, J.H. Lee, C.W. Won, Mater. Res. Bull. 38 (2002) 1135–1146.
[13] H.H. Nersisyan, J.H. Lee, S.I. Lee, C.W. Won, Combustion and flame, 2003, in print.
[14] P. Zivanovich, R. Curcich, G. Djurkovich, V. Jokanovich, D. Uskokovich, Int. J. SHS 10 (2001) 91–99.
[15] J. Zhang, J.H. Lee, D.Y. Maeng, C.W. Won, J. Mater. Sci. 36 (2001) 3233–3238.
[16] J.B. Holt, US patent number 4,944,930, July 31, 1990.
[17] V.V. Zakorzhevskii, I.P. Borovinskaya, Int. J. SHS 9 (2000) 171–191.
[18] E.G. Gilan, R.B. Kaner, Chem. Mater. 8 (1996) 333–343.
[19] I.P. Parkin, Chem. Soc. Rev. 25 (1996) 199–208.
[20] A.A. Shiryaev, Int. J. SHS 4 (1995) 351–355.
[21] A.A. Zenin, A.G. Merzhanov, H.H. Nersisyan, Dokl. Akad. Nauk SSSR 250 (1980) 880–884 (in Russian).
[22] A.A. Zenin, A.G. Merzhanov, H.H. Nersisyan, Combust., Explos., Shock Waves 1 (1981) 79–86.
[23] J.B. Zeldovich, D.A. Frank-Kamenetsky, J. Phys. Chem 12 (1938) 100–105 (in Russian).